UNIVERSITY TWENTE

Ultra-thin PbTiO3 films – thickness and ferroelectricity

Sander W. Logtenberg

22-02-2013

Abstract

The ferroelectric properties of epitaxial $PbTiO_3$ thin films with thickness < 15 nm have been studied. The films were grown on $SrTiO_3$ (001) substrates with $SrRuO_3$ bottom electrodes using pulsed laser deposition. Growth was monitored down to the deposition of individual monolayers using reflection high-energy electron diffraction. Piezoresponse force microscopy was used to study the ferroelectric response of the perovskites thin films. Using film thicknesses ranging from 5.9 to 14.6 nm $PbTiO_3$ it was found that the thin films show a clear ferroelectric response down to 9.0 nm.

Table of Contents

Abstract 1

Literature study - Ferroelectric properties and critical size 3

Ferroelectricity 3

Size reduction in ferroelectrics 3

Critical size 4

Motivation 6

Hypothesis 6

Techniques used 6

Pulsed Laser Deposition (PLD) &Reflection high-energy electron diffraction (RHEED) 6

Piezoresponse Force Microscopy (PFM) 7

X-Ray Reflectivity 7

Substrate preparation 7

Results 10

Sample 1 – 14.6 nm 10

Sample 2 – 6.2 nm 13

Sample 3 – 5.9 nm 16

Sample 4 – 9.0 nm 17

Discussion 19

Conclusion 20

Recommendations 20

REFERENCES 21

Literature study - Ferroelectric properties and critical size

Ferroelectricity

A ferroelectric is a material that has an intrinsic spontaneous polarization that can be reversed by applying an external electrical field greater than the coercive field (1). All ferroelectrics are also pyroelectric and all pyroelectrics are also piezoelectric. The piezoelectric property allows for piezoresponse force microscopy to be used to determine ferroelectricity in a sample made from ferroelectric material. A typical piezoresponse graph should look roughly like figure 2, which shows different domain responses for +10 and -10 V indicating that the ferroelectric polarization has been reversed.

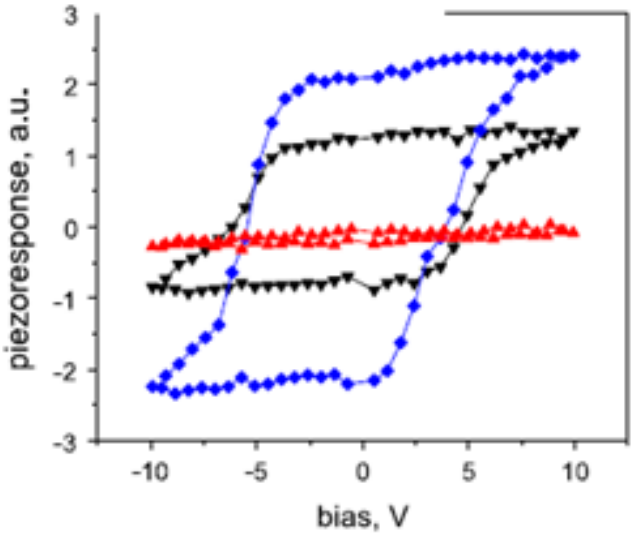

Figure 2) Piezoresponse measured with PFM, $BiFeO_3$ (blue), $CoFe_2O_3$ (black) and a $BiFeO_3$ – $CoFe_2O_3$ heterostructures (red) (7)

Ferroelectrics have many potential uses so a lot fo studies are dedicated to this group of materials (21-25); however, with a 'typical' coercive field of 50 kV/cm any ferroelectric device is required to be very small to be applicable in silicon chips, i.e. 1 micrometer for a 5 V voltage requirement (1). One of the applications for ferroelectrics is data storage, where smaller sized material is extremely beneficial in order to put as much data in as little space as possible.

Size reduction in ferroelectrics

Lead titanate, ($PbTiO_3$, or PTO) and its ferroelectric domains has been the subject of many studies (14-19). Uniformly polarized, or monodomain, PTO films show an increase in the depolarization field strength for smaller film thicknesses as well as a reduction of the film tetragonality c/a (2). The depolarization field and other surface phenomena have been the subject of several studies (12), in particular with regards to superlattices (12, 13). For very small sizes however, a polydomain structure forms (3) and the tetragonality starts to recover to its initial value. Figure 3 shows this tetragonality recovery as well as a significant difference for PTO grown on an electrode layer of $La_{0.67}Sr_{0.33}MnO_3$ on insulating $SrTiO_3$ (STO) and PTO grown directly on a conducting substrate, Nb-STO.

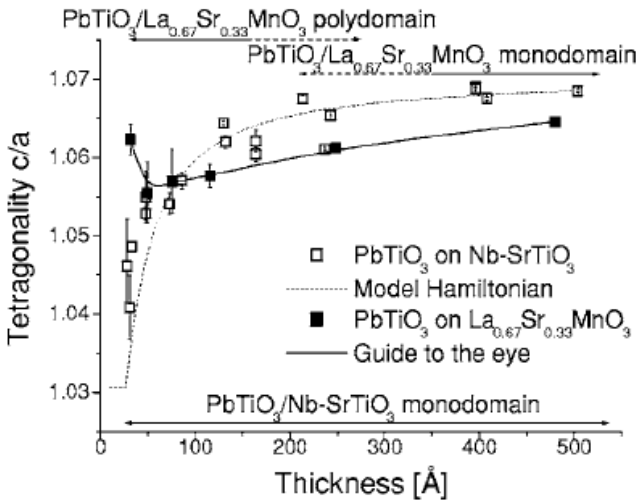

Fig 3) Tetragonality as a function of film thickness in PTO, grown in conducting Nb-STO (open squares) and PTO grown on $La_{0.67}Sr_{0.33}MnO_3$ electrodes on insulating STO substrates (black squares) (2)

Lichtensteiger et al (2) researched the transition from mono- to polydomain structure for thin films, showing polydomain behavior in films with a thickness of 249 Å and lower (fig 4). This transition occurs to reduce the electric field energy from the depolarization field (5).

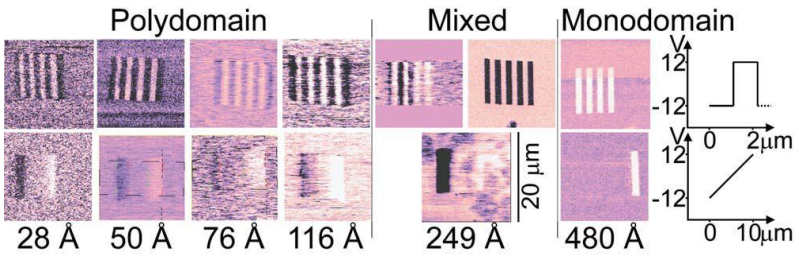

Fig 4) Piezoresponse after alternate −12 and +12 V voltages were applied (top) and piezoresponse after gradually ramping a voltage from -12 to +12 V (bottom) (2)

Critical size

PTO thin films show ferroelectric behavior for very small sizes. Over time, many models have predicted a certain critical size, below which ferroelectricity would theoretically not be possible. However, practical work and more recent models have consistently shown a decrease in predicted critical size. Figure 4 shows ferroelectricity in PTO films down to 28 Å, grown using off-axis magnetron sputtering, on 200-300 Å electrodes deposited on insulating STO substrates. Six years earlier however, a first principle model by Ghosez and Rabe in 2000 (4) shows that PTO films as thin as 12 Å, or three unit cells, would still show ferroelectric behavior. Four years later, Fong et al (5) have grown PTO films of 1-4 unit cells thick using metalorganic chemical vapor deposition on 001 STO substrates. Using diffuse x-ray scattering (figure 5) Fong et al confirmed ferroelectric behavior down to 3 unit cells, and paraelectric behavior for smaller films. Finally, in 2010 Shimada et al showed in an ab initio study that it is possible that films of 1 and 2 unit cell thicknesses can have stable ferroelectric domains as well (20), suggesting that no critical thickness exists.

In 2009, Han et al (6) published a paper detailing piezoresponse in PTO thin films and nanoislands, using pulsed laser deposition (PLD) to create the films and chemical solution deposition to create the

islands. At 10 nm thickness, both the thin films and the islands showed no piezoresponse. Unfortunately the article doesn't specify which substrate was used. A few different substrates are mentioned but none in direct correlation to the thin films and islands.

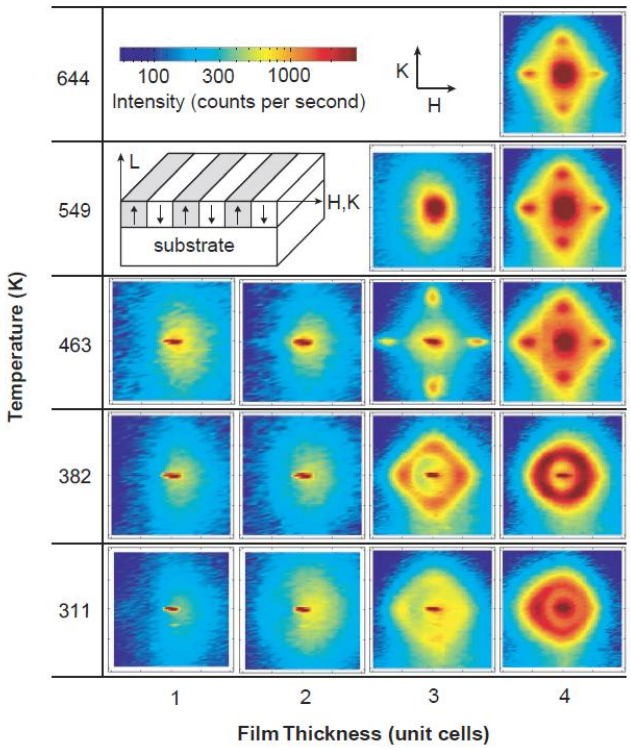

Fig 5) In-plane diffuse x-ray scattering around the PTO (303) Bragg peak, showing satellites from ferroelectric stripe domains for film thicknesses of 3 and 4 unit cells (5)

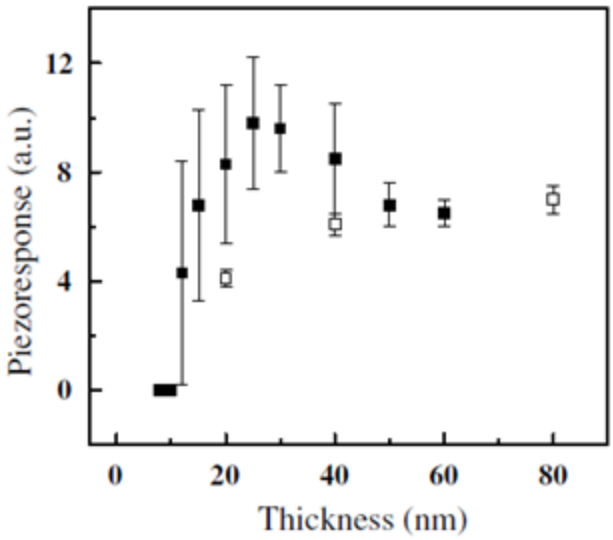

Fig 6) Piezoresponse versus thickness of nanoislands (solid squares) and thin films (open squares) (6)

Motivation

Pulsed laser deposition (PLD) is an established technique for the deposition of thin films with near-perfect stoichiometry. Using reflection high-energy electron diffraction (RHEED) the growth can be monitored down to a single monolayer, allowing for the deposition of ultrathin films. While PTO films have been shown to be ferroelectric down to 3 unit cells, those were grown using deposition techniques other than PLD. Not many studies have used PLD to investigate the ferroelectric properties of PTO films with thicknesses of 10 nm or less. In an attempt to study these properties, this thesis will be utilizing piezoresponse force microscopy to investigate ultra-thin PTO films grown on STO (001) substrates. Since these substrates are insulating, an electrode layer is necessary. Using pulsed laser deposition, ultra-thin PTO films will be grown on ~ 20 nm $SrRuO_3$ (SRO) acting as bottom electrode layer on insulating single terminated (001) STO substrates. Various PTO thicknesses will be used in order to find the critical thickness below which no ferroelectricity can be found.

Hypothesis

Pulsed laser deposition can be used to successfully produce ultrathin $PbTiO_3$ films that show ferroelectric properties for thicknesses down to three unit cells.

Techniques used

Pulsed Laser Deposition (PLD) &Reflection high-energy electron diffraction (RHEED)

The samples were prepared with pulsed laser deposition, using the PLD LTRHEED MASIF system.

Setting \ **Material**	**$SrRuO_3$**	**$PbTiO_3$**
Heater temperature (^oC)	650	600
Laser power (mJ)	46	46
Oxygen pressure (mbar)	0.120	0.120
Pre-ablation	300 pulses, 5 Hz	300 pulses, 5 Hz
Laser fluence (J/cm^2)	2.03	2.03
Spot size (mm^2)	1.5	1.5
Mask area (mm^2)	99	99
Window efficiency	90 %	90 %
Distance target to substrate (mm)	50	50
Scan area (mm)	5.0 (width) x 1.0 (height)	5.0 (w) x 1.0 (h)
Scan speed (mm/s)	0.2	0.2
Deposition laser frequency (Hz)	1	1
Annealing pressure (mbar)	n/a	100

Each sample contains roughly 20 nm of SRO electrode deposited on the substrate.

RHEED measurements were taken at 30 V and roughly 1.3 A. The current requires some calibration though, meaning that the first 30-60 seconds of most measurements don't show clear oscillations yet because the correct current has to be found. This is made harder by the fact that the surface becomes very rough as soon as deposition starts, reducing the output intensity greatly. Alignment was done by showing a diffraction pattern on the camera (fig 7).

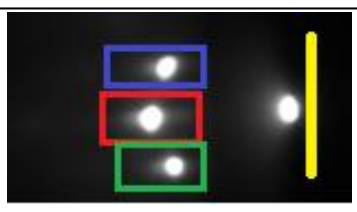

Fig 7) RHEED camera alignment; sample (yellow) and the three different diffraction peaks (red, blue, green) that are measured and plotted

The RHEED output consists of a graph plotting peak intensity of the three diffraction spots (red, blue and green plots respectively) versus elapsed time. Each oscillation on this graph should represent the growth of one monolayer of material. Using the lattice constant for PTO (a=3.904 Å at room temperature) the film thickness can be determined. The pattern is also relevant because it can indicate a 2D growth pattern (10). Figure 8a shows the desirable RHEED pattern from a perfect STO substrate. The pattern on the dotted line indicates a flat or 2D surface. The arrows point out the Kikuchi lines, which indicate that the surface is flat and crystalline. Figure 8b shows the RHEED pattern expected from a rough 3D surface. This could indicate that islands have formed on the substrate instead of a flat surface, indicating that there is bad or no bonding between the substrate and the film (10).

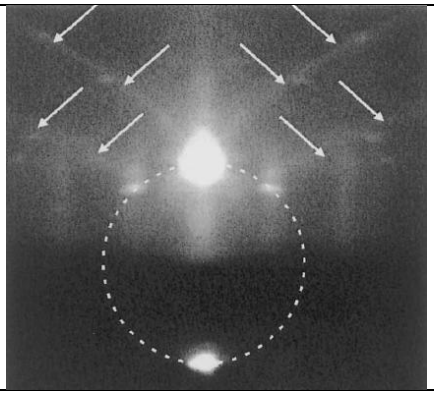

Fig 8 a) RHEED pattern from a TiO_2 terminated (001) STO substrate (10)

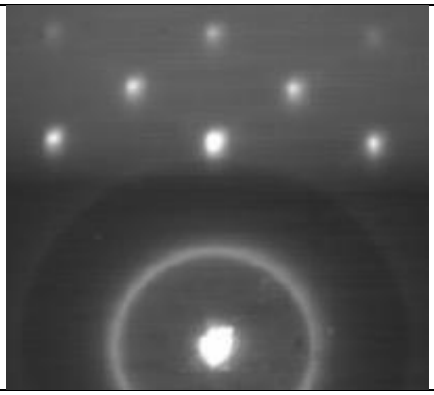

b) RHEED pattern from a rough 3D surface (11)

Piezoresponse Force Microscopy (PFM)

The piezoresponse was measured using the Bruker Dimension Icon. The sample was grounded, and either a bias voltage was applied to the tip to show domain switching or a voltage ramp was used to show a piezoresponse loop similar to fig 2.

X-Ray Reflectivity

To confirm the thickness of some of the samples the Bruker D8 XRD was used. Alignment was done using 1.0 mm slits, measurements sometimes used smaller ones. The reflectivity was measured in a locked coupled scan, starting at θ=0.2 (and 2θ=0.4) up to θ=6 at increments of 0.001 at 0.1 sec/step.

Substrate preparation

Treatment of substrate single crystals is crucial for optimized growth of complex perovskites like SRO (27). STO (001) single crystals were subjected to pre-established treatment procedure in order to obtain B-site (TiO_2) termination (28). As received substrates were cleaned using acetone and ethanol. Afterwards they were treated in an ultrasonic bath in DI water for half an hour in order to hydrolyze the strontium oxide. Water reacts with strontium oxide to form strontium hydroxide, which in turn was etched using buffered hydrofluoric acid in the next step. This removed the A-site (SrO) terminations from the substrate surface and made the entire surface B-site terminated. Finally, the

substrates were cleaned and annealed in furnace at 900 ^{0}C for 90 minutes with an oxygen flow of 150 liter per hour.

Using the Bruker Dimension Icon for atomic force microscopy (AFM) the surface topography of the treated substrates was checked (fig 9, 10). Using the program Gwyddion, a profile plot was made (fig 11) From the graph it can be noticed that the difference in height between individual surface steps is ~ 0.4 nm, corresponding to one unit cell of cubic STO lattice and this confirms the surface was B-site terminated after the treatment procedure.

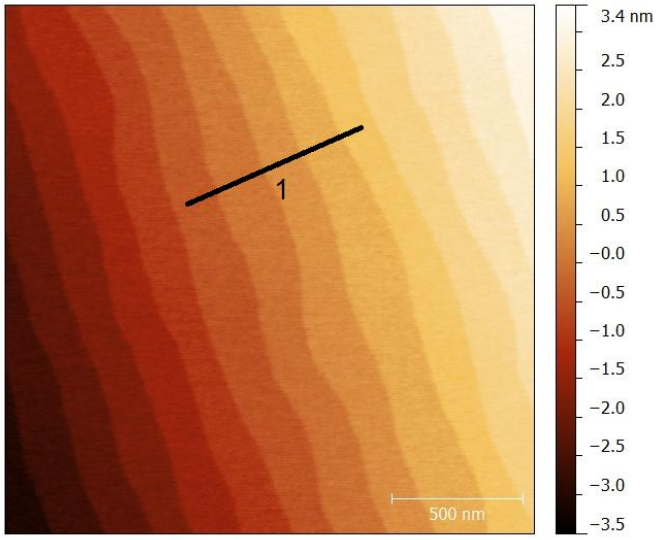

Fig 9) AFM height sensor

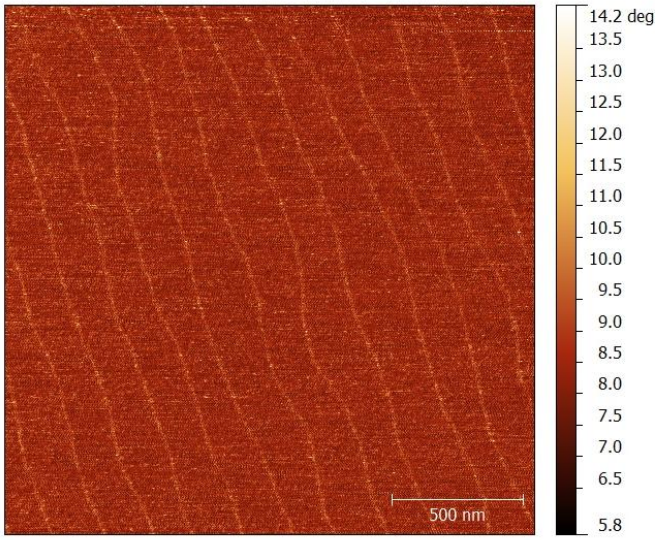

Fig 10) AFM amplitude sensor

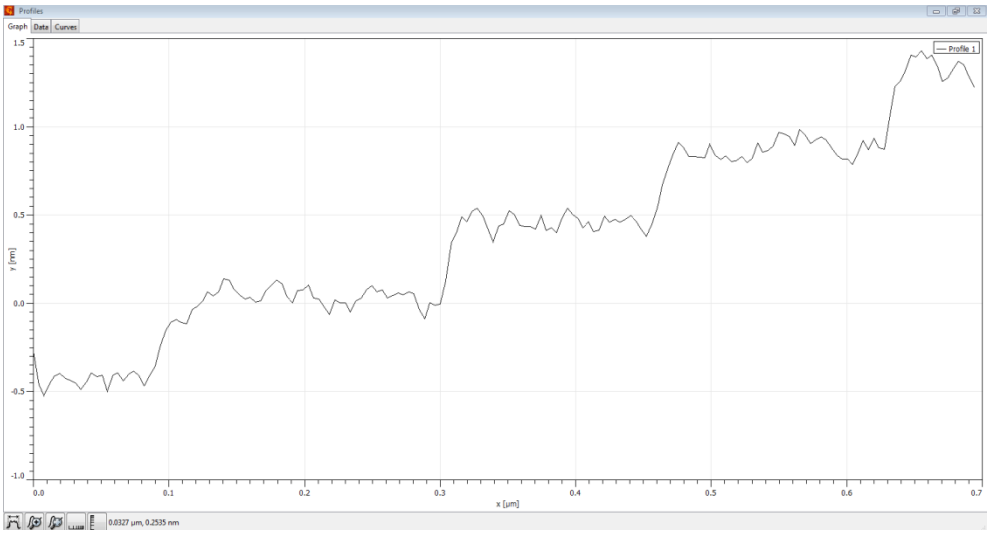

Fig 11) AFM profile plot

Results

Sample 1 – 14.6 nm

Because in-situ RHEED studies could not be performed, X-Ray reflectivity was employed to determine the thickness of this sample. The θ-2θ scan (fig 12) shows oscillations due to density differences between different layers. A FFT of the θ-2θ scan (fig 12) shows two peaks; the first one indicates the thickness of PTO at 14.6 nm (fig 13), and the second peak indicates the thickness of the SRO at 19.9 nm.

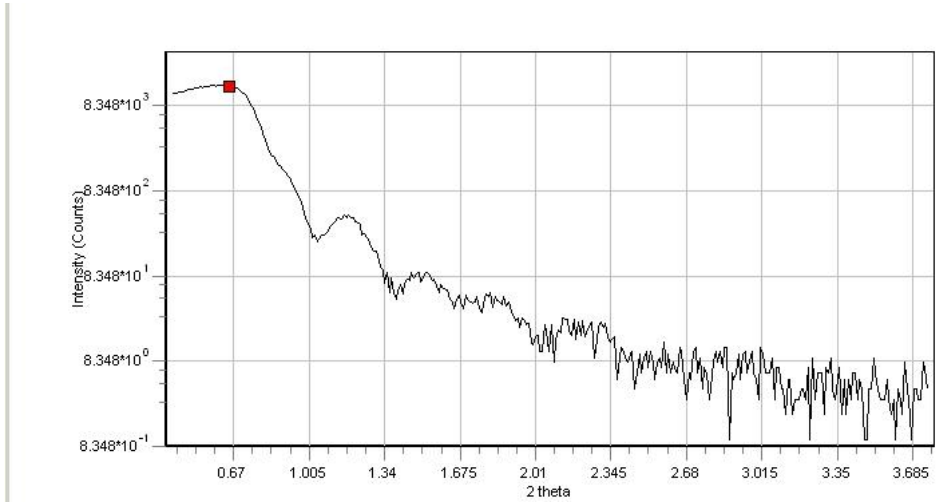

Fig 12) θ-2θ scan

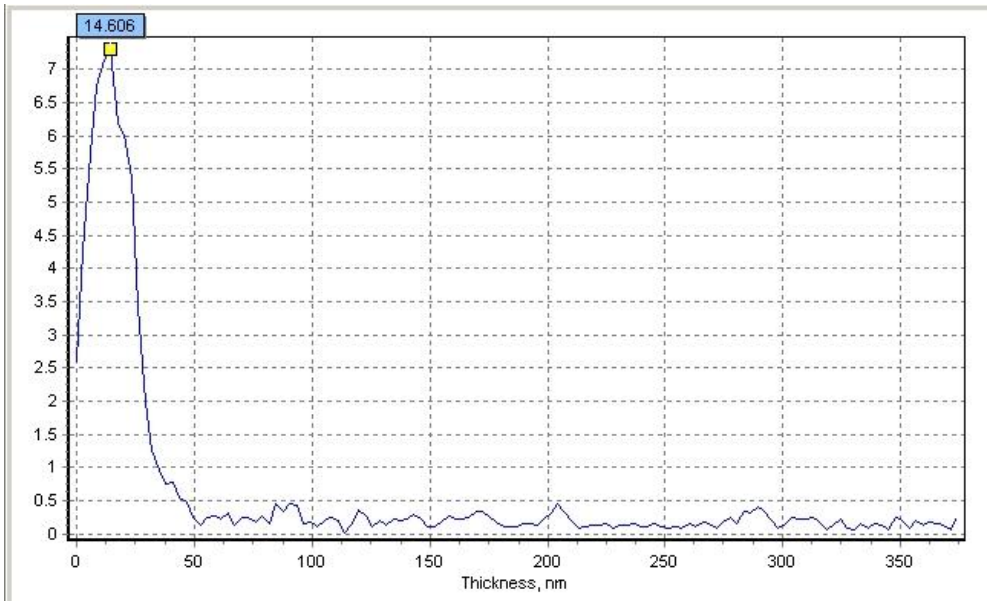

Fig 13) FFT of the scan result in fig 12, showing the PTO thickness at 14.6 nm

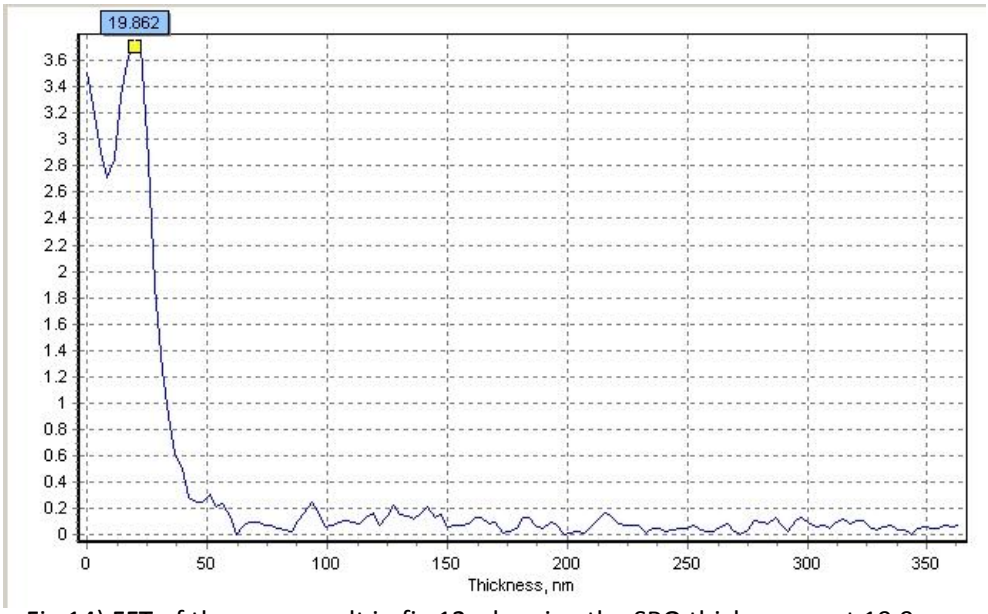

Fig 14) FFT of the scan result in fig 12, showing the SRO thicknesses at 19.9 nm

The film was subjected to study using the PFM. A sweeping voltage of -6V to +6 V DC was applied through the PFM tip. The results of this voltage ramp (fig 15) shows an 180^0 phase difference between -4 V and +4 V, indicating that the ferroelectric polarization of the material has been switched between the up and the down polarization.

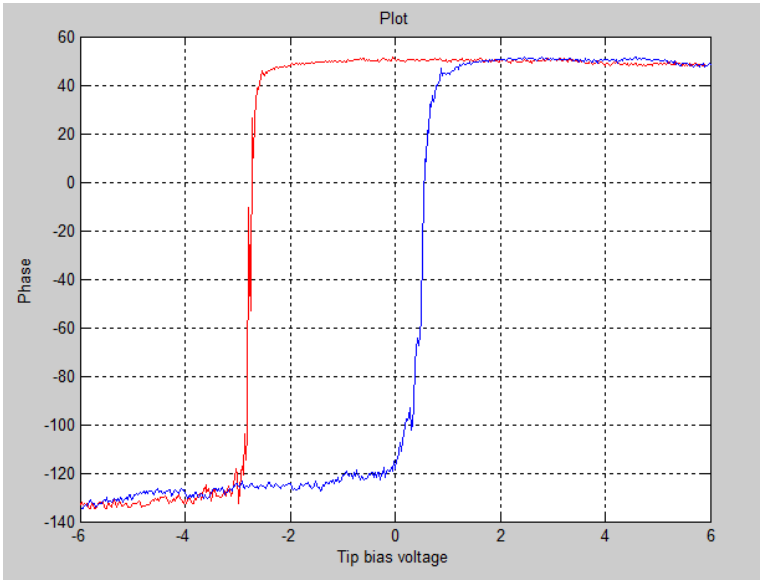

Fig 15) Piezoresponse phase as a function of bias voltage applied to 14.6 nm thick PTO
Ramp up (red) and ramp down (blue)

Figure 16 and 17 represent phase and amplitude response respectively after a +4 V DC was applied on 2*2 µm area of 14.6 nm thick PTO film. Clear difference in contrasts of the phase response inside and outside the area of applied bias voltage indicates switching of ferroelectric domains. The area outside the switching shows uniform contrast in both phase and amplitude response, so it can be concluded that this film consisted of a single domain. This is remarkable, since the research from Lichtensteiger et al (fig 3, (2)) predicts that a film of this thickness would show polydomain behavior rather than monodomain.

Due to the prominent ferroelectric response, this sample will be used as a reference to compare the following thinner films to.

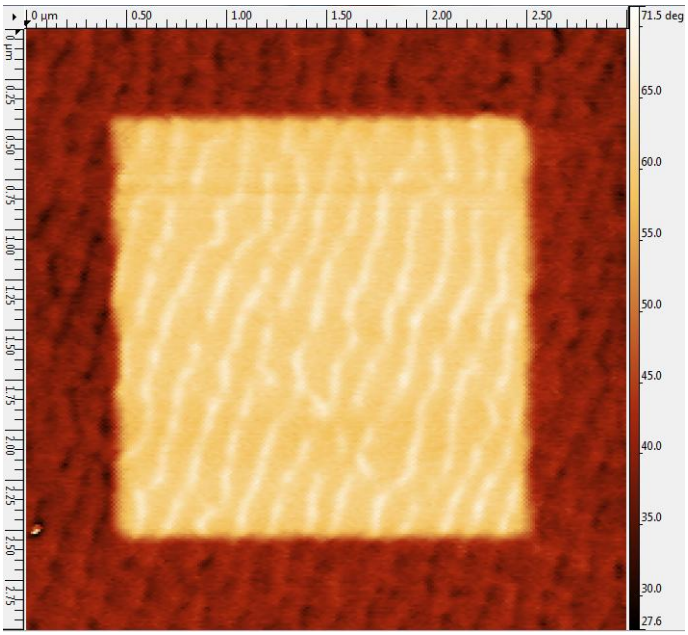

Fig 16) Piezoresponse phase after switching 14.6 nm thick PTO

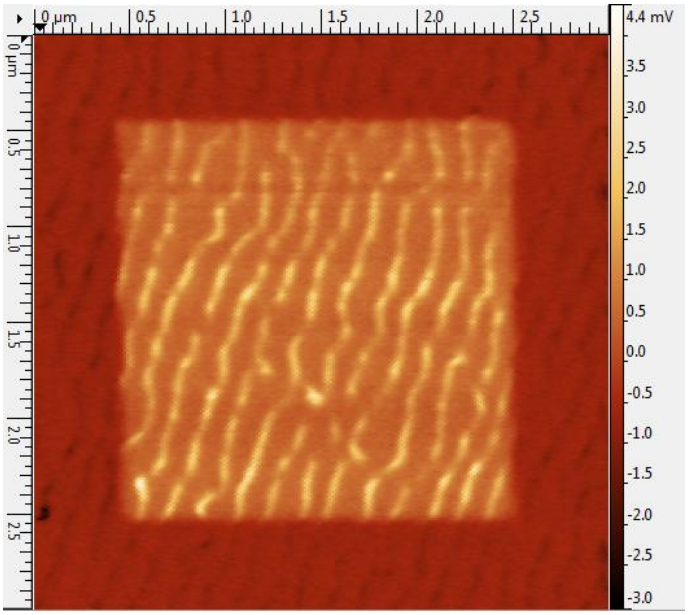

Fig 17) Piezoresponse amplitude after switching 14.6 nm thick PTO

Sample 2 – 6.2 nm

The sample with a thickness of 6.2 nm was deposited over the course of 300 seconds with 300 laser pulses. The electron reflection (fig 18) shows oscillations consistent with layer by layer growth of about 16 monolayers, corresponding to a thickness of 6.2 nm. The RHEED intensity profile shows that the intensity of the electron beam gradually decreases with increasing thickness of the PTO film. This indicates that the surface roughness increased over the course of the deposition. The last portion of the graph (after 300 seconds) shows a steady increase in peak intensity due to smoothening of the surface and the crystal structure forming.

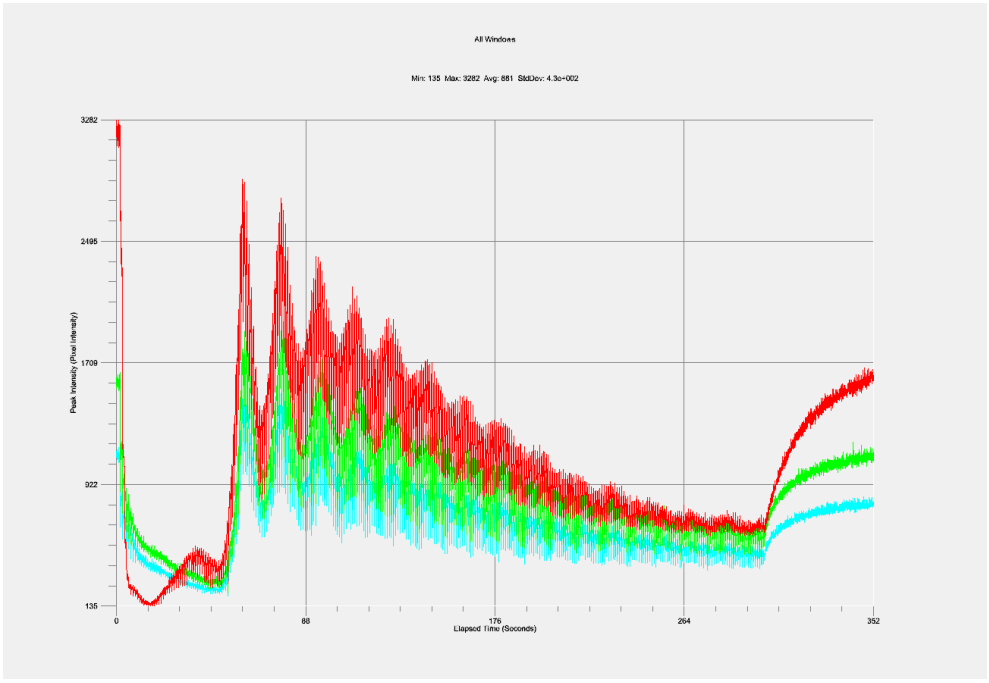

Fig 18) RHEED oscillations, 300 seconds growth indicating 6.2 nm thick PTO

Figure 19 shows the RHEED camera images, indicating 2D surfaces and growth.

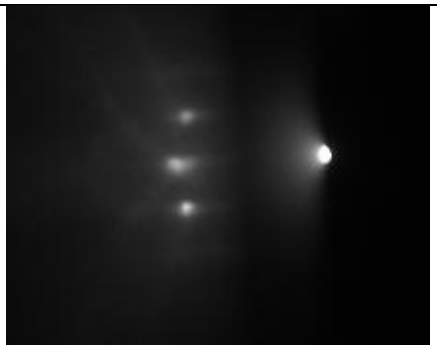

Fig 19 a) Substrate

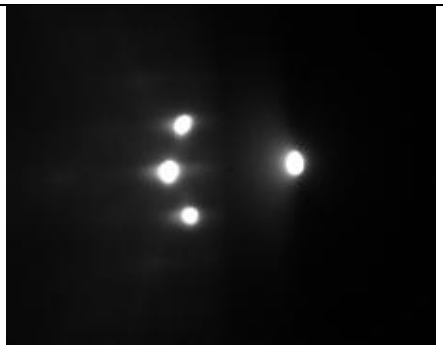

b) After SRO

c) After PTO

The PFM voltage ramp is shown in figure 20. The graph shows that the difference between the minimum and maximum phase is only 3^0. It is unlikely that this is an actual ferroelectric response from the material, but rather the result of some surface charge effect or water molecules interfering with the measurement.

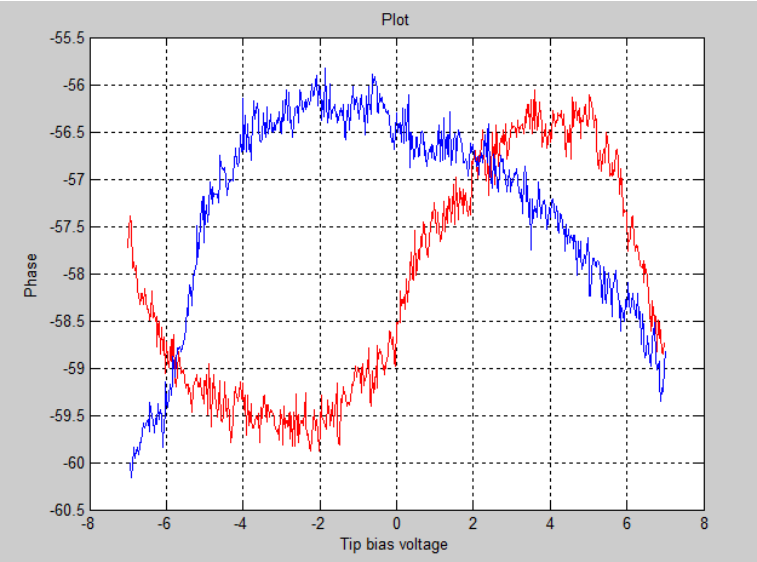

Fig 20) Piezoresponse phase as a function of bias voltage, applied to 6.2 nm thick PTO Ramp up (red) and ramp down (blue)

Just like the 14.6 nm thick film, a DC voltage was applied in order to show a ferroelectric domain switch. This procedure resulted in some response from the material, but unlike the 14.6 nm thick film the switching is not as prominent, as shown in figure 21 and 22. The attempted switch area can be made out between 0.5 and 1.5 µm and shows some bright spots that could indicate that some small islands have indeed been switched.

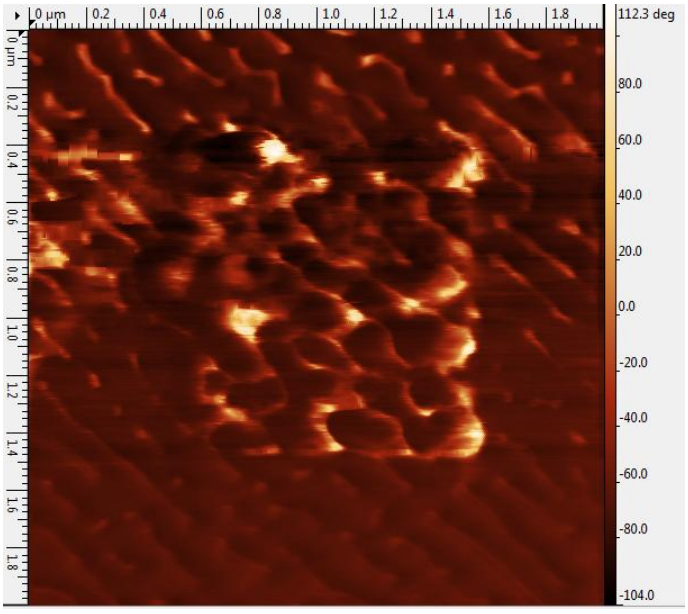

Fig 21) Piezoresponse phase after switching 6.2 nm thick PTO

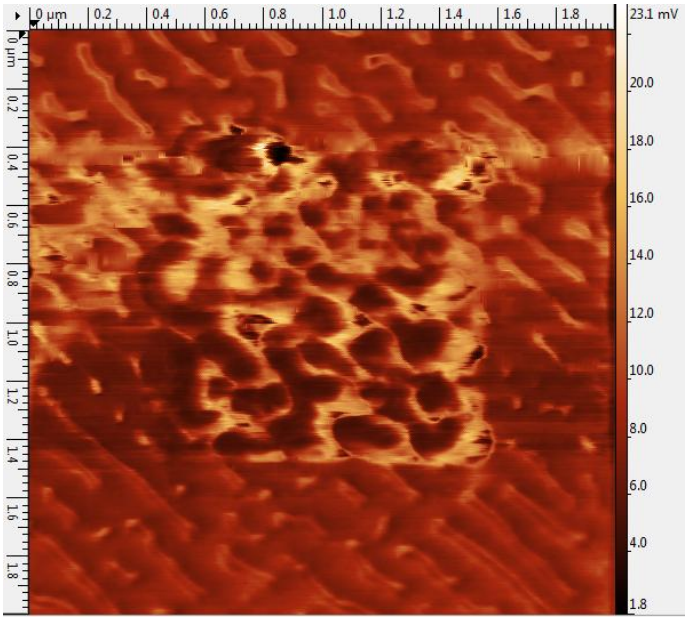

Fig 22) Piezoresponse amplitude after switching 6.2 nm thick PTO

The height sensor (fig 23) tells a different story however. It shows that the target area has been deformed by the switching, something that was found to be prominent when applying negative voltages. This deformation would also cause the phase and amplitude response to register incorrectly, thus invalidating those results.

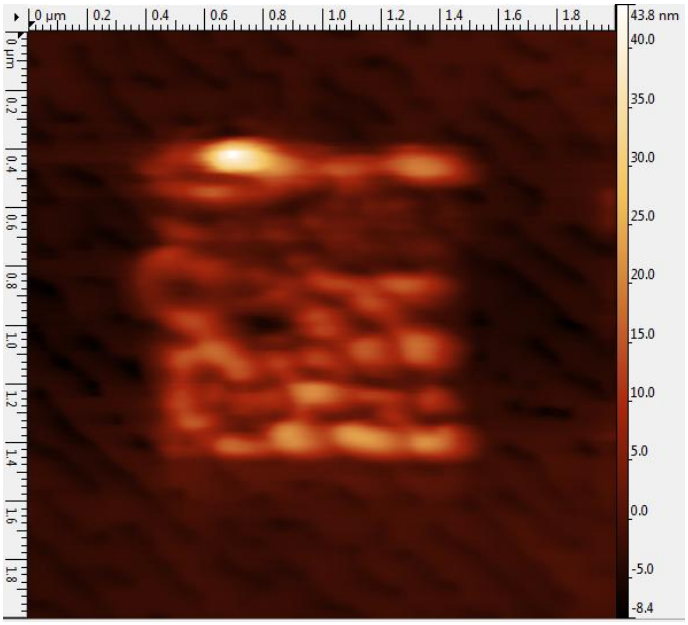

Fig 23) Piezoresponse height sensor after switching 6.2 nm thick PTO

Sample 3 – 5.9 nm

The thinnest sample with a thickness of 5.9 nm was deposited over the course of 360 seconds with 360 laser pulses. The RHEED oscillations (fig 24) show the growth of 15 monolayers, corresponding to 5.9 nm film thickness. The RHEED intensity profile shows a much smaller decrease over time compared to the 6.2 nm deposition, which would indicate that the film surface is less rough. There is a significant difference in growth rate between the 6.2 nm and 5.9 nm films, since the thinnest one was grown with 60 pulses more. The growth rate of the films will be discussed later on.

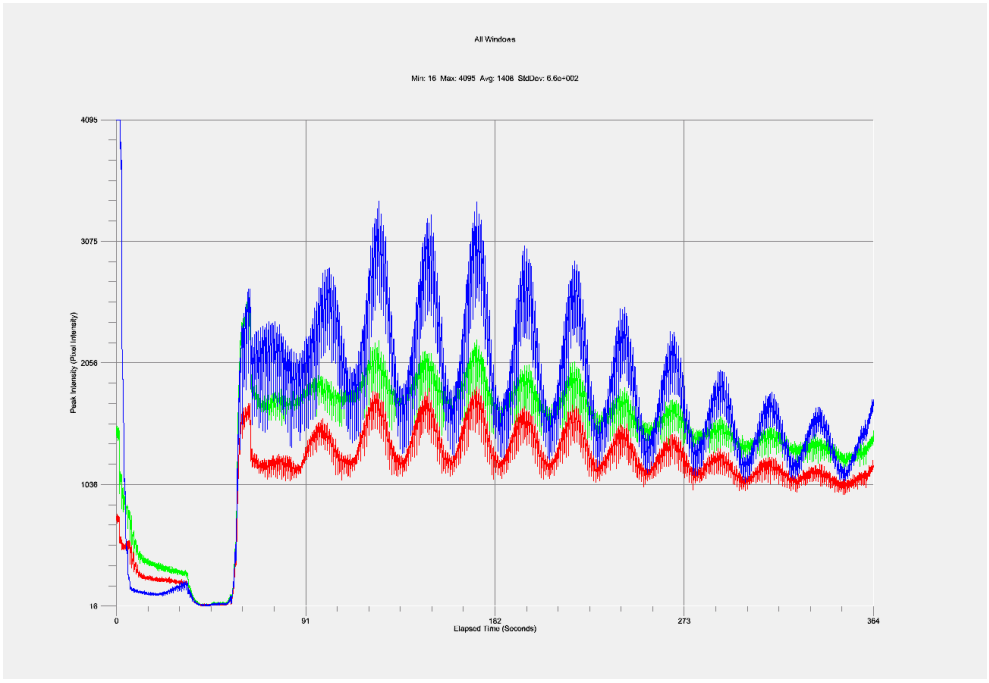

Fig 24) RHEED oscillations, 360 seconds growth indicating 5.9 nm thick PTO

This sample shows no piezoresponse to speak of. Compared to the 14.6 nm film the phase response (fig 25) shows nothing like an 180^0 domain switch.

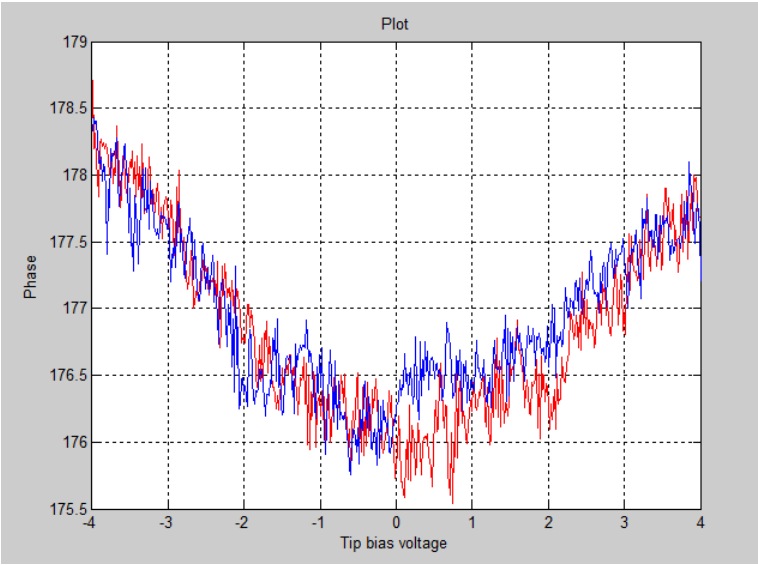

Fig 25) Piezoresponse phase as a function of bias voltage, applied to 5.9 nm thick PTO
Ramp up (red) and ramp down (blue)

Sample 4 – 9.0 nm

Since the thinner samples showed none of the desired ferroelectric properties, a thicker film was needed. The 9.0 nm sample was deposited over the course of 600 seconds with 600 laser pulses. The RHEED oscillations (fig 26) show 23 monolayers, corresponding to 9.0 nm film thickness. Like the 6.2 nm film RHEED oscillations (fig 18) the profile of figure 26 indicates increased surface roughness for increased PTO thickness, as well as the forming of the crystal structure after the deposition.

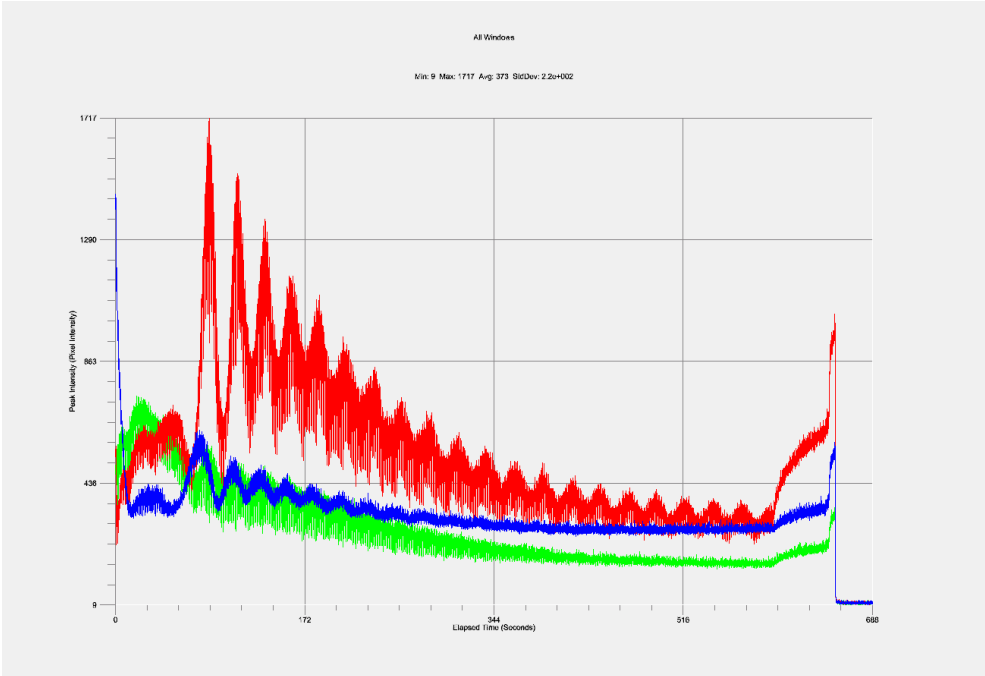

Fig 26) RHEED oscillations, 600 seconds growth indicating 9.0 nm thick PTO

The RHEED camera images (fig 27) again show 2D growth for the SRO electrode. The substrate reflection looks very similar to figure 8a, indicating a perfect substrate.

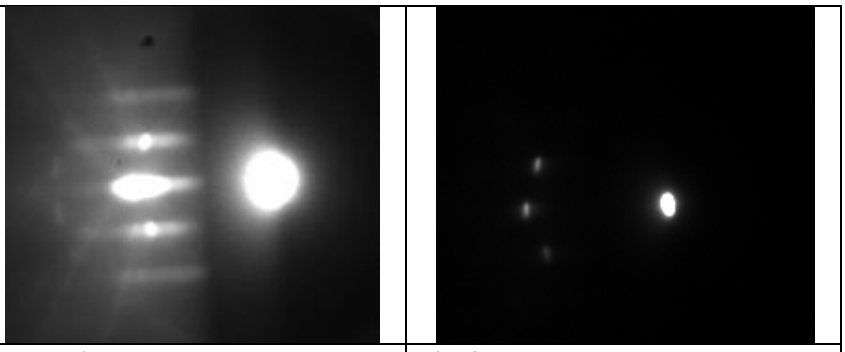

Fig 27 a) Substrate	b) After SRO

This sample definitely shows a piezoresponse (fig 28) although it is not as clean as the 14.6 nm film. While figure 28 shows an 180^0 switch, there is a lot more noise compared to figure 15. Most notably, the graph goes wild between -2 and -4 V. This could be due to an oscillation effect or a deformation similar to what the height sensor in figure 23 shows.

In addition, the 9.0 nm graph shows its maximum at low voltage and its minimum at high voltage, which is the reverse compared to the 14.6 nm sample. This could be due to the spontaneous polarization of the material; Dahl et al (8) have shown that PTO films thinner than 20 nm predominantly have a polarization toward the SRO electrode, while thicker films tend to spontaneously polarize toward the top surface. Alternatively, the PFM measurement arbitrarily mixes up the ramp up and ramp down results.

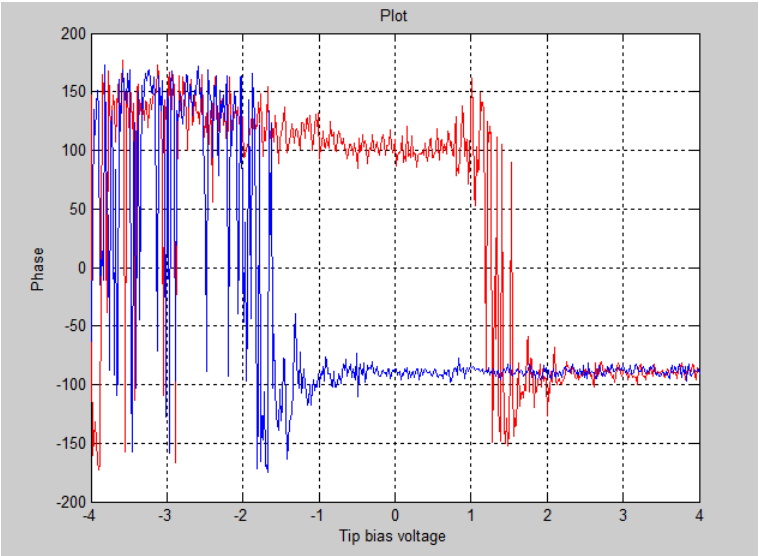

Fig 28) Piezoresponse phase as a function of bias voltage, applied to 9.0 nm thick PTO Ramp up (red) and ramp down (blue)

Discussion

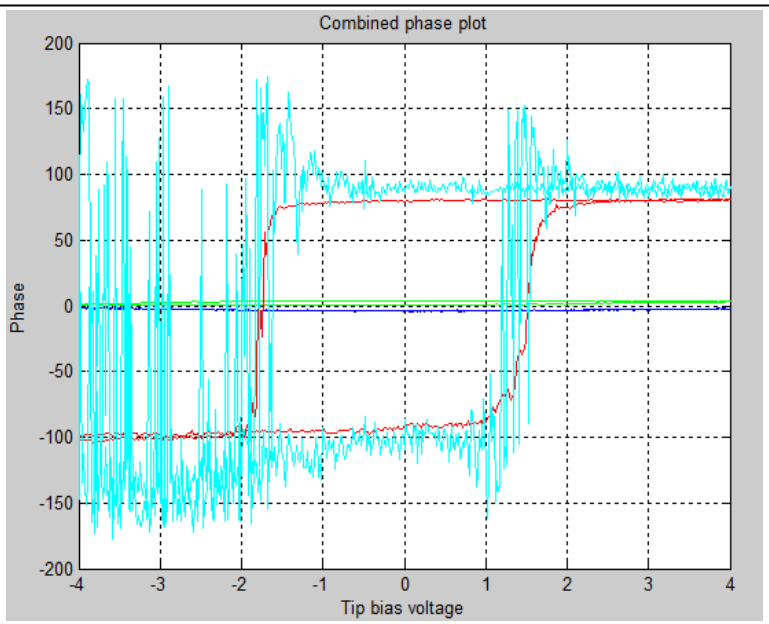

Fig 29) Combined phase plot; 14.6 nm thick PTO (red), 6.2 nm (green), 5.9 nm (blue) and 9.0 nm (cyan)

Figure 29 shows a combined plot of the phase responses of the different thicknesses, normalized for easy comparison. The graphs were centered around (0,0) and the 9.0 nm film response was reversed to allow for easy comparison to the 14.6 nm (red) graph.
The 14.6 nm (fig 29, red) and 9.0 nm (fig 29, cyan) films are the only samples that shows a 180^0 domain switch, a piezoresponse phase loop similar to the expected loop shown in figure 2. Both the 5.9 nm film (fig 29, blue) and 6.2 nm (fig 29, green) show no response whatsoever and an attempt to switch an area of the 6.2 nm film (fig 20) resulted in deformation rather than ferroelectric switching. It is clear from the height sensor that the sample was damaged when a -6 V switch was attempted. Due to time constraints, no successful switch of the 9.0 nm film was done.

The RHEED graphs of figure 18 (6.2 nm), 24 (5.9 nm) and 26 (9.0 nm) show different growth rates, namely 1.25, 0.976 and 0.898 nm per minute respectively. This could be due to any variable being off, such as slightly lower or higher oxygen pressure during deposition, variance in laser power transmission due to a variation in window efficiency (since the laser power is measured outside the PLD system the transmission through the window could be slightly different for different depositions). Alternatively, the distance from the target to the substrate could accidentally have been higher for the lower growth rates.

Another notable phenomenon is the trenches that are clearly visible all over the PFM area scans (fig 16, 17, 20, 21, 22). According to Koster et al (9) the trenches are formed by uneven growth of the SRO layer; referring to a very similar sample of 30 nm SRO on a STO substrate it is stated that despite the TiO_2 termination, Sr would diffuse to the surface and move to the step edges. The trenches are then formed because the $SrRuO_3$ grows more slowly on the SrO-terminated areas compared to the TiO_2-terminated areas. The uneven growth of SRO then also causes trenches in the PTO layer.

The results presented here show that it is possible to use pulsed laser deposition to acquire ferroelectric PTO films of 9.0 nm, a thickness below the 10 nm that was found in the literature study. While several articles have shown that PTO films can be ferroelectric down to 3 unit cells, those studies used different deposition techniques than PLD in addition to different methods of characterization. The two smaller samples of 5.9 and 6.2 nm thicknesses showed very little to no

ferroelectric response, despite showing very good RHEED oscillations. It is possible that the growth conditions, while optimized for the RHEED oscillations, are not perfect for the ferroelectric properties of the material. Alternatively there is a flaw in the use of the PFM for characterization.

Conclusion

Using pulsed laser deposition $PbTiO_3$ films of different thickness less than 15 nm were deposited using optimized growth conditions. RHEED oscillations corresponding to deposition of individual monolayers were obtained for PTO growth up to 23 unit cells. The ferroelectricity in these ultrathin films was probed using piezoresponse force microscopy (PFM). The thinnest PTO film showing ferroelectricity was found to be 9.0 nm thick. While (001) epitaxial PTO films with less than 9nm thickness were shown to still be ferroelectric in literature, this study obtained it as the minimum thickness of ferroelectricity on (001) STO substrates using a particular set of growth conditions.

Not all the possible data was collected due to time constraints, such as switching of the 5.9 and 9.0 nm samples using the PFM. Results presented in this thesis mainly focused on obtaining layer-by-layer growth of PTO under PLD deposition conditions. The results can help further studies on PTO thin films providing good growth conditions suitable for layer-by-layer growth; however, the growth conditions and parameters should be optimized to approach further downscaling in thickness while maintaining the ferroelectricity. There can be several possible angles of approach to study further epitaxial PTO thin films that have not been tried out which are discussed in the Recommendations section below.

Recommendations

Further downscaling is required, and the tetragonality of those films should be studied in addition to measuring the piezoresponse since the literature suggests that these two properties are connected. Another future goal is to reduce not only the thickness, but the other dimensions as well, i.e. using lithography to create nanostructures, and measure the piezoresponse and domain morphology of those structures.

Another angle of approach that could yield different results would be using a conductive substrate and no electrode layer, since figure 3 does show that films behave differently in each case.

Although thicknesses much smaller have been reported in the literature than could be achieved here, further studies are necessary to reveal the key deposition factors. Most importantly, growth conditions should be looked at and where possible optimized for ferroelectric properties. PLD is a very promising technique, but using the current growth conditions it does not appear to be holding up against other deposition techniques. Characterization methods should be studied as well; the PFM method may yield different results from i.e. in-plane diffuse x-ray scattering, the method used to find the 3 unit cell critical thickness.

REFERENCES

(1) Applications of Modern Ferroelectrics, J. F. Scott, *Science* 315, 954 (2007); doi: 10.1126/science.1129564

(2) Monodomain to polydomain transition in ferroelectric PbTiO3 thin films with La0.67Sr0.33MnO3 electrodes, C. Lichtensteiger, M. Dawber; N. Stucki; J. M. Triscone, J. Hoffman, J. B. Yau, C. H. Ahn, L. Despont and P. Aebi; Appl. Phys. Lett. 90, 052907 (2007); doi: 10.1063/1.2433757

(3) Scaling of structure and electrical properties in ultrathin epitaxial ferroelectric heterostructures, V. Nagarajan, J. Junquera, J. Q. He, C. L. Jia, R. Waser, K. Lee, Y. K. Kim, S. Baik, T. Zhao, R. Ramesh, Ph. Ghosez and K. M. Rabe; J. Appl. Phys. 100, 051609 (2006); doi: 10.1063/1.2337363

(4) Microscopic model of ferroelectricity in stress-free PbTiO3 ultrathin films, Ph. Ghosez and K. M. Rabe; Appl. Phys. Lett. 76, 2767 (2000); doi: 10.1063/1.126469

(5) Ferroelectricity in Ultrathin Perovskite Films, D. D. Fong, G.B. Stephenson, S.K. Streiffer, J.A. Eastman, O. Auciello, P.H. Fuoss and C. Thompson; Science 304, 1650 (2004); doi: 10.1126/science.1098252

(6) Fabrication of epitaxial nanostructured ferroelectrics and investigation of their domain structures, H. Han, K. Lee, W. Lee, M. Alexe, D. Hesse and S. Baik; J Mater Sci (2009) 44:5167–5181 doi: 10.1007/s10853-009-3528-2

(7) Spatially resolved mapping of ferroelectric switching behavior in self-assembled multiferroic nanostructures: strain, size, and interface effects, B. J. Rodriguez, S. Jesse, A. P. Baddorf, T. Zhao, Y. H. Chu, R. Ramesh, E. A. Eliseev, A. N. Morozovska and S. V. Kalinin; 2007 Nanotechnology 18 405701 doi: 10.1088/0957-4484/18/40/405701

(8) Polarization direction and stability in ferroelectric lead titanate thin films, Ø. Dahl, J. K. Grepstad, and T. Tybell; J. Appl. Phys. 106, 084104 (2009); doi: 10.1063/1.3240331

(9) Structure, physical properties, and applications of SrRuO3 thin films, G. Koster, L. Klein, W. Siemons, G. Rijnders, J. S. Dodge, C.-B. Eom, D. H. A. Blank, M. R. Beasley, Rev. Mod. Phys. 2012, 84, 253. DOI: 10.1103/RevModPhys.84.253

(10) Thin films and heterostructures for Oxide Electronics, Ch. 12, p 355-384, G. Rijnders and D. H. A. Blank

(11) http://research.physics.unc.edu/project/ftsui/mbe/RHEED.html

(12) New phenomena at the interfaces of very thin ferroelectric oxides, M. Dawber, N. Stucki, C. Lichtensteiger, S. Gariglio and J. M. Triscone, J. Phys.: Condens. Matter 20 (2008) 264015 (6pp)
doi: 10.1088/0953-8984/20/26/264015

(13) Unusual Behavior of the Ferroelectric Polarization in PTO-STO Superlattices, M. Dawber, C. Lichtensteiger, M. Cantoni, M. Veithen, P. Ghosez, K. Johnston, K. M. Rabe, and J.M. Triscone, PRL 95, 177601 (2005)
doi: 10.1103/PhysRevLett.95.177601

(14) Microscopic model of ferroelectricity in stress-free PbTiO3 ultrathin films, Ph. Ghosez and K. M. Rabe, Appl. Phys. Lett. 76, 2767 (2000)
doi: 10.1063/1.126469

(15) Diffraction contrast analysis of 90 and 180 deg ferroelectroc domain structures of PTO thin films, K. Aoyagi, T. Kiguchi, Y. Ehara, T. Yamada, H. Funakubo and T. J. Konno, Sci. Technol. Adv. Mater. 12 (2011) 034403 (6pp)
doi: 10.1088/1468-6996/12/3/034403

(16) X-ray diffraction of ferroelectric nanodomains in PTO thin films, G. Catalan, A. H. G. Vlooswijk, A. Janssens, G. Rispens, S. Redfern, G. Rijnders, D. H. A. Blank & B. Noheda; Integrated Ferroelectrics: An International Journal, 92:1, 18-29 (2007)
doi: 10.1080/10584580701746707

(17) Investigation of ferroelectricity in Ultrathin $PbTiO_3$ Films, C. Lichtensteiger and J. M. Triscone; Integrated Ferroelectrics: An International Journal, 61:1, 143-148 (2004)
doi:10.1080/10584580490459062

(18) Ferroelectric stripe domains in PTO thin films: depolarization field and domain randomness; R. Takahashi, Ø. Dahl, E. Eberg, J. K. Grepstad, and T. Tybell, JOURNAL OF APPLIED PHYSICS 104, 064109 (2008)
doi: 10.1063/1.2978225

(19) Imaging and alignment of nanoscale 180° stripe domains in ferroelectric thin films; C. Thompson, D. D. Fong, R. V. Wang, F. Jiang, S. K. Streiffer, K. Latifi, J. A. Eastman, P. H. Fuoss, and G. B. Stephenson, Applied Physics Letters 93, 182901 (2008)
doi: 10.1063/1.3013512

(20)Ab initio study of ferroelectric closure domains in ultrathin PTO films, T. Shimada, S. Tomoda and T. Kitamura, Physical Review B 81, 144116 (2010)
doi: 10.1103/PhysRevB.81.144116

(21) Self-organization nanodomain structure in ferroelectric ultrathin films, Z. Wu, W. Duan, N. Huang, J. Wu and B. Gu, Nanotechnology 18 (2007) 325703 (4pp)
doi: 10.1088/0957-4484/18/32/325703

(22) Fundamental size limits in ferroelectricity, N. A. Spaldin, Science 304, 1606 (2004);
doi: 10.1126/science.1099822

(23) Phase transitions in nanoscale ferroelectric structures, S. K. Streiffer and D. D. Fong, MRS Bulletin V 34 I 11 pp 832-837 (2009)
doi: 10.1557/mrs2009.233

(24) Phase transitions in ultra-thin ferroelectric films and fine period multilayers, M. Dawber, C. Lichtensteiger and J. Triscone, Phase Transitions: A Multinational Journal, 81:7-8, 623-642 (2008)
doi: 10.1080/01411590802048315

(25) Thickness dependence of polarization in ferroelectric perovskite thin films, G. Liu and C. Nan, J. Phys. D: Appl. Phys. 38 (2005) 584–589
doi:10.1088/0022-3727/38/4/010

(26) Curie temperature and critical thickness of ferroelectric thin films, B. Wang and C. H. Woo, J. Appl. Phys. 97, 084109 (2005)
doi: 10.1063/1.1861517

(27) Enhanced surface diffusion through termination conversion during epitaxial SrRuO3 growth, G. Rijnders, D.H.A. Blank, J. Choi, C.B. Eom, Applied Physic Letters 84 (2004) 505-507
doi: 10.1063/1.164047

(28) Quasi-ideal strontium titanate crystal surfaces through formation of Sr-hydroxide, G.Koster, B.L.Kropman, A.J.H.M.Rijnders, D.H.A. Blank, H.Rogalla, Applied Physics Letters 73 (1998) 2020-2922
doi: 10.1063/1.122630

Abbreviations used

PTO – Lead titanate – $PbTiO_3$
STO – Strontium titanate – $SrTiO_3$
SRO – Strontium ruthenate – $SrRuO_3$
PFM – Piezoresponse Force Microscopy
PLD – Pulsed Laser Deposition
RHEED – Reflection High-Energy Electron Diffraction